

Article

## Effects of Nano-MnO<sub>2</sub> on Dopaminergic Neurons and the Spatial Learning Capability of Rats

Tao Li <sup>1,2,†</sup>, Tingting Shi <sup>2,†</sup>, Xiaobo Li <sup>1</sup>, Shulin Zeng <sup>2</sup>, Lihong Yin <sup>1</sup> and Yuepu Pu <sup>1,\*</sup>

<sup>1</sup> Key Laboratory of Environmental Medicine Engineering, Ministry of Education, School of Public Health, Southeast University, Nanjing 210009, China; E-Mails: llg501@aliyun.com (T.L.); lixiaobo1007@hotmail.com (X.L.); lhyin@seu.edu.cn (L.Y.)

<sup>2</sup> Institute of Neurobiology, Southeast University, Nanjing 210009, China; E-Mails: shitingting.student@sina.com (T.S.); zsl@seu.edu.cn (S.Z.)

† These authors contributed equally to this work.

\* Author to whom correspondence should be addressed; E-Mail: yppu@seu.edu.cn; Tel.: +86-25-8379-4996; Fax: +86-25-8327-2583.

Received: 24 June 2014; in revised form: 16 July 2014 / Accepted: 25 July 2014 /

Published: 6 August 2014

---

**Abstract:** This study aimed to observe the effect of intracerebrally injected nano-MnO<sub>2</sub> on neurobehavior and the functions of dopaminergic neurons and astrocytes. Nano-MnO<sub>2</sub>, 6-OHDA, and saline (control) were injected in the substantia nigra and the ventral tegmental area of Sprague-Dawley rat brains. The neurobehavior of rats was evaluated by Morris water maze test. Tyrosine hydroxylase (TH), inducible nitric oxide synthase (iNOS) and glial fibrillary acidic protein (GFAP) expressions in rat brain were detected by immunohistochemistry. Results showed that the escape latencies of nano-MnO<sub>2</sub> treated rat increased significantly compared with control. The number of TH-positive cells decreased, GFAP- and iNOS-positive cells increased significantly in the lesion side of the rat brains compared with the contralateral area in nano-MnO<sub>2</sub> group. The same tendencies were observed in nano-MnO<sub>2</sub>-injected rat brains compared with control. However, in the the positive control, 6-OHDA group, escape latencies increased, TH-positive cell number decreased significantly compared with nano-MnO<sub>2</sub> group. The alteration of spatial learning abilities of rats induced by nano-MnO<sub>2</sub> may be associated with dopaminergic neuronal dysfunction and astrocyte activation.

**Keywords:** nano-MnO<sub>2</sub>; Morris water maze; dopaminergic neurons; glial fibrillary acidic protein

---

## 1. Introduction

Manganese (Mn) is an abundant, naturally occurring element in the Earth's crust. In organisms, Mn is a cofactor of several enzymes, such as transferases, hydrolases, lyases, arginase, glutamine synthetase, and superoxide dismutase; Mn is also found in integrins [1]. Considering the dependence of multiple enzymes on Mn, this element is essential for various physiological processes, such as modulation of the immune system, stellate process production in astrocytes, cell adhesion, and protein and carbohydrate metabolism [2–5]. Although Mn is essential for metabolic functions, excessive exposure to Mn is a well-recognized occupational hazard. Occupational exposure to Mn for six months to two years can cause an extrapyramidal syndrome, referred to as manganism, which exhibits symptoms similar to idiopathic Parkinson's disease at molecular and clinical levels [6–8].

Nano-sized materials are novel substances rapidly developed and usually measured as 1 to 100 nm size in one dimension. At a nanometer scale, the surface area increases rapidly as particle size decreases, as a result, the electromagnetic, optical, thermal, and mechanical properties of nanomaterials change. With the rapid development of nanotechnology and extensive application of nanomaterials, the health effects of nanoparticles on human body, particularly on the nervous system, have been widely investigated [9,10]. In electrochemical [11] and environmental fields [12], nano-MnO<sub>2</sub> is a novel material that increases the exposure to Mn during production and application. Due to the potential application in biomedical imaging fields [13,14], the exposure risk of human beings to manganese-based magnetic nanoparticles also increased. In medical applications, these nanoparticles can be injected *in vivo*. Further, nanomaterials can enter the body via the respiratory tract; for example, welding fumes generally contain Mn metal and manganese oxide particles, therefore, welders have high exposure risk [15], and the deposition of Mn in the brain areas of welders is extensive enough to produce a magnetic resonance imaging (MRI) response [16]. These materials can also enter the body by gastrointestinal absorption and dermal contact; some nanomaterials enter the central nervous system [17] via the bloodstream or nasal olfactory nerve endings. It is known that increased manganese (Mn) exposure causes neurotoxic effects, like cognitive, psychiatric and motor deficits *in vivo* [16]. The long-term and low-dose Mn exposure induced dopaminergic impairment [18], this condition may be associated with intracellular oxidative stress, mitochondrial damage, and protein aggregation [19], and alteration of glia components in brain [20]. Studies also showed that Mn poisoning exhibits similar molecular alterations, motor behaviors, and nervous system symptoms to Parkinson's syndrome at early stages [21]. With the increasing exposure potential, neurotoxicology of nano-MnO<sub>2</sub> should be assessed in terms of bio-security.

In the present experiment, nano-MnO<sub>2</sub> was injected in the rat brain with the aid of a stereotaxic instrument to investigate the neurotoxicity of nano-MnO<sub>2</sub>. 6-Hydroxydopamine (6-OHDA) was used as a positive control treatment and saline was administered as a negative control treatment. Nano-MnO<sub>2</sub>-induced behavioral effects on rats were investigated using Morris water maze experiments.

Changes in tyrosine hydroxylase (TH) and glial fibrillary acidic protein (GFAP) expressions were analyzed by immunohistochemistry.

## 2. Experimental Section

### 2.1. Reagents and Instruments

The following substances were used in this study: nano-MnO<sub>2</sub> (diameter = 10 nm; concentration = 87 µg/µL; Amresco, Solon, OH, USA); 6-OHDA; apomorphine (APO), mouse anti-rat TH monoclonal antibody and polyclonal rabbit anti-rat GFAP antibody (Sigma, Saint Louis, MO, USA). General-purpose chain enzyme peroxidase-labeled avidin (SP-9000) immunohistochemistry kit (Beijing Zhongshan Golden Bridge Biotech, Beijing, China) and concentrated DAB color kit (ZLI-9032; Beijing Zhongshan Golden Bridge Biotech) were also used.

The following instruments and systems were also used: stereotaxic apparatus (Jiangwan II, Shanghai Second Military Medical University, Shanghai, China); Morris water maze and video systems RD1101-MM (Shanghai Yishu Info. Tech., Shanghai, China); freezing microtome (CM-1900, Leica, Wetzlar, Germany); optical microscope (Olympus, Nagano, Japan); and image processing system (Leica).

### 2.2. Experimental Designs

Forty rats were screened by a training phase of Morris water maze test, then the two rats which had extremely short and the two which had extremely long escape latencies were removed. The remaining 36 rats were randomly grouped (12 rats per group) as nano-MnO<sub>2</sub>-, 6-OHDA-, and saline-treated groups. Following the intracerebral injection, Rotation behaviors of rats were detected. 7 and 14 days after injection, Morris water maze test were performed to observe the cognitive capability of rats (12 rats per group on 7 day, 8 rats per group on 14 day). 7, 14 and 28 days after injection, the expression of TH, GFAP and iNOS were detected in rats brain (4 rats per group for each time point) tissue by immunohistochemistry.

### 2.3. Animal Experiments

Male Sprague-Dawley rats (200 g to 250 g; Experimental Animal Center of Southeast University) were housed with equal daily periods of light and dark cycles and provided free access to food and water. The animal protocols used in this work were conducted in accordance with the Declaration of Helsinki, and approved by Ethics Committee of Southeast University (Project identification No. 201105012).

The rats were anesthetized with 0.4% sodium pentobarbital (40 mg/kg body wt., i.p.), fixed in the stereotaxic apparatus, and subjected to conventional disinfection and craniotomy. The bregma was exposed by creating a top middle skin incision. The injection targets were the substantia nigra pars compact (SNc) and the ventral tegmental area (VTA), which were identified according to Paxinos-Watson atlas of rat [22]. The SNc injection point coordinates (mm) were as follows: AP, -4.8; ML, 1.8; DV, 9.2. The VTA injection point coordinates (mm) were as follows: AP, -4.8; ML, 1.0; and DV, 9.2. Approximately 1 µL of 87 µg/µL nano-MnO<sub>2</sub>, 1 µL of 9 µg/µL 6-OHDA solution, or 1 µL of

solvent (0.9% NaCl) was injected at a rate of 0.5  $\mu\text{L}/\text{min}$  using a 5  $\mu\text{L}$  microsyringe. The needle was retained for 5 min after injection, withdrawn 0.5 mm, then the needle was retained at this position for another 5 min, withdrawn slowly at a rate of 2.0 mm/min. Afterward, the rats were kept warm and fed when they were conscious.

#### 2.4. Rotation Behavior

The severity of dopamine depletions was evaluated by assessments of rotational behavior. To measure nanoparticles induced behavioural lesion, the animals were injected with 0.05 mg/kg APO one week after exposure. The number of rotations ipsilateral and contralateral to the lesion during a 40-min interval after APO injection was recorded.

#### 2.5. Morris Water Maze Test

A Morris water maze test was performed before injection as training phase. The diameters of the water maze and the platform were 160 and 11 cm, respectively. The platform was placed at a fixed location in the center of one of the four imaginary quadrants. Three starting points were set at the midpoint in round basin of the imaginary quadrants except the one where the platform was located. Twenty mL of ink was added to the water to form an opaque solution at  $25 \pm 1$  °C. Visual cues outside the water maze were relatively fixed. For the training experiment, the rats were released at one of the three different starting positions. The rats were allowed to spend 180 s to find the hidden escape platform in water and stayed there for 10 s. If the rats could not find the platform within 180 s, the experimenter helped them locate this platform and the rats stayed there for 10 s. Continuous training was performed four times a day for 4 days and 24 h after the last training session, rats were injected. Seven days and 14 days after injection, the rats were released from one of the starting positions, which was opposite to the quadrants where the platform was, four times and allowed to swim for up to 120 s. Distance travelled, swim speed and escape latency were measured in each trial.

#### 2.6. Immunohistochemical Staining

After the Morris water maze test was conducted, the rats were anesthetized with 0.4% sodium pentobarbital (40 mg/kg body wt., i.p.) and perfused intracardially with 400 mL of 4% paraformaldehyde. The brains were removed and post-fixed in 4% paraformaldehyde for 24 h and stored in 30% sucrose solution. The middle brain was obtained for continuous coronal slicing (30  $\mu\text{m}$ ). Immunohistochemical staining steps were summarized as follows: (1) the slices were cooled to room temperature, washed with PBS (pH 7.4; 0.01 mol/L) twice for 5 min, and incubated in 3%  $\text{H}_2\text{O}_2$  for 15 min; (2) the slices were washed thrice with PBS for 5 min; 10% goat serum working solution was then added at 37 °C for 30 min without washing; (3) anti-TH (1:10,000), iNOS(1:100) and GFAP (1:80) were added at 4 °C and stored overnight; (4) the slices were washed with PBS thrice for 5 min; biotin-labeled secondary antibody working solution was added at 37 °C for 60 min; (5) the slices were washed again with PBS thrice for 5 min; alkaline phosphatase-labeled streptavidin was added at 37 °C for 30 min; (6) the slices were washed again with PBS thrice for 5 min and stained with DAB; double-distilled water was used to terminate the reactions; (7) PBS was placed in the patch, dehydrated, transparent,

and mounted. Another slice was used as a negative control sample, in which normal goat serum was used instead of the primary antibody.

After immunostaining, the brain sections were examined under light microscopy by two histologists blinded to treatment conditions. The immunoreactivities of TH, GFAP and iNOS were evaluated. The number of TH<sup>+</sup>, GFAP<sup>+</sup> and iNOS<sup>+</sup> cells of each rat brain section was counted in three nonoverlapping high-power fields (HPFs; 400× magnification) and analyzed. The HPFs were selected from hippocampal areas for GFAP, SNc and VTA regions for TH and iNOS that had a maximum of positive cells. In each studied field, only positive cells with the nucleus at the focal plane were counted.

### 2.7. Statistical Analysis

Indicators of the Morris water maze tests were analyzed by ANOVA, followed by student's *t* test for parametric comparison between groups. The immunostaining results were statistically analyzed by ANOVA, followed by Student's *t* test or nonparametric *t* test statistics. Results are shown as arithmetic means and standard errors of means. SPSS 13.0 software was used for statistical analysis, and the significance level was set at  $p < 0.05$ .

## 3. Results and Discussion

### 3.1. Motor Behavioral Study

The rats showed *in situ* rotation from head to tail with center of the injection-contralateral hindlimb one week after exposure and 5 min after APO injection in 6-OHDA treatment group. In the nano-MnO<sub>2</sub> group, no head-to-tail rotation was observed after injection, but abnormal behaviors, such as tremors, slow activity, sniffing, irritability and vertical tail, were shown. Mn dust exposure also induces these Parkinson-like symptoms [19]. Our result suggested a slight extrapyramidal impairment, but the typical Parkinson's symptom, which is the head-to-tail rotation, was not observed.

### 3.2. Morris Water Maze Test

Morris water maze test results are shown in Table 1. The escape latencies of nano-MnO<sub>2</sub>- and 6-OHDA-treated rats showed a significant increase compared with those in the saline group (\*  $p < 0.05$ , \*\*  $p < 0.01$ ) both 7 and 14 days after injection, however, the escape latencies in the 6-OHDA group was significantly longer than that in nano-MnO<sub>2</sub>-treated group 14 days after injection. The velocity of 6-OHDA-treated rats also showed a significant decrease compared with the saline group (\*  $p < 0.05$ ).

Mn exposure showed adverse effects on cognition capability. In rodents, the hippocampus is a structure responsible for spatial navigation [23,24]. Hippocampal place cells are orientation-invariant and location-specific, and are mainly located in CA1 and CA3 region of hippocampus [24,25]. Two weeks of intranasal manganese chloride exposure induced spatial memory deficits in rats [26]. High-manganese diet also results in behavioral deficits of rats in the Morris water maze tests [27]. Our results suggested that nano-MnO<sub>2</sub> impair the spatial learning of rats, while when compared with the positive control, 6-OHDA, showed less toxic effects. Other nanoparticles may affect neurobehaviors once the central nervous system is contaminated. Zinc oxide nanoparticles extend the

escape latency of mice in the Morris water maze test [28]. Maternal exposure to titanium dioxide nanoparticles during lactation period can also cause impairments on learning and memory ability of rat offspring [29]. These cognitive impairments are associated with damage to the hippocampus.

**Table 1.** Escape latency and score of rats in Morris water maze test ( $\bar{x} \pm s$ ).

	7 Days after Injection			14 Days after Injection		
	Saline	6-OHDA	Nano-MnO <sub>2</sub>	Saline	6-OHDA	Nano-MnO <sub>2</sub>
Escape latencies (s)	27.62 ± 28.73	64.68 ± 43.62 **	63.89 ± 42.73 **	25.12 ± 29.03	67.69 ± 51.61 **	60.52 ± 41.24 <sup>##,***</sup>
Velocity (cm/s)	24.81 ± 4.35	19.28 ± 3.77 *	21.59 ± 3.61	23.75 ± 3.69	18.72 ± 4.65 *	21.64 ± 3.32

<sup>#</sup>  $p < 0.05$ , <sup>##</sup>  $p < 0.01$ , compared with 6-OHDA group; \*  $p < 0.05$ , \*\*  $p < 0.01$ , compared with saline group.

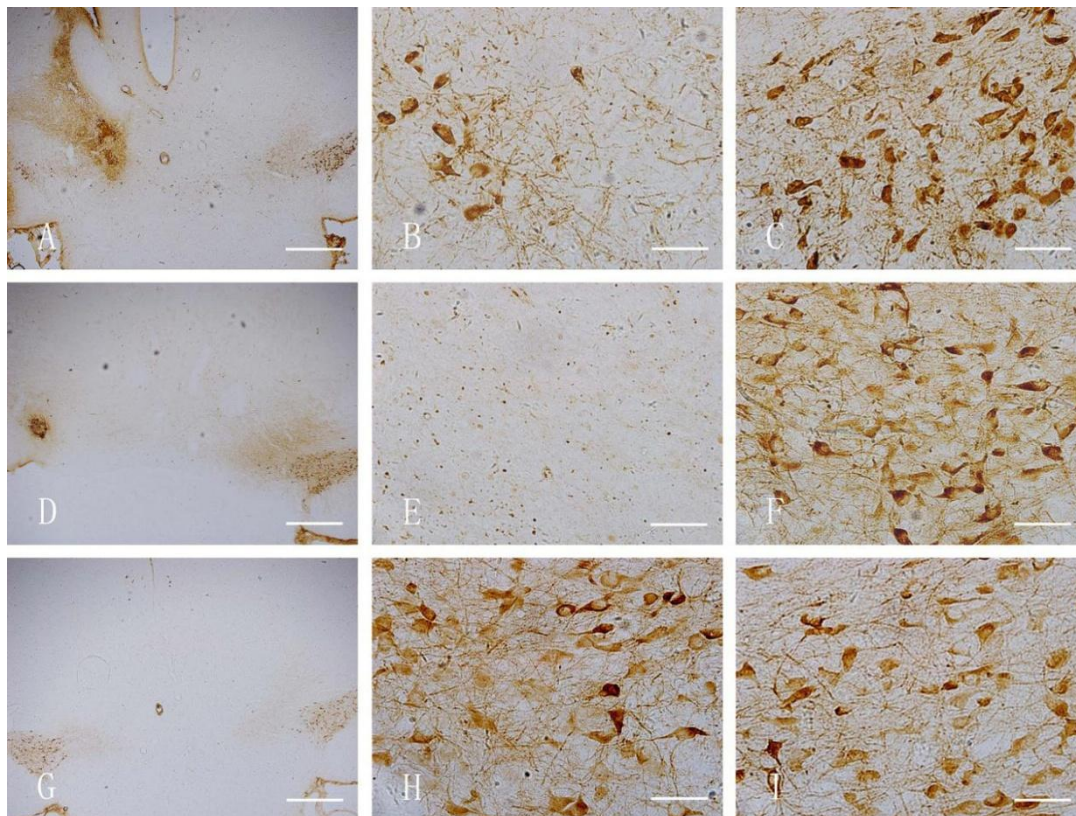
For the 7 days after injection Morris water maze test,  $n = 12$ ; 14 days after injection Morris water maze test,  $n = 8$ .

### 3.3. Immunohistochemical Staining

Figure 1 shows the TH-stained rat brains. In both the nano-MnO<sub>2</sub> and 6-OHDA groups, TH-positive cells on the damaged sides (B, E) were significantly less than those of the contralaterals (C, F) and the damaged side of the saline group (H) at 7 d after injection. Figure 2 shows the GFAP-stained hippocampus of the rats. In both the nano-MnO<sub>2</sub> and 6-OHDA groups, GFAP-positive cells on the damaged side (A, C) were significantly higher than those of the contralaterals (B, D) and the damaged side of the saline control (E, F) at 7 days after exposure. Figure 3 also shows the rat brains subjected to iNOS immunohistochemical staining. In nano-MnO<sub>2</sub> and 6-OHDA groups, iNOS-positive cells on damaged sides (A, C) were significantly higher than those of the contralaterals (B, D) and damaged sides of the saline group (E) one week after injection. The number of TH-, GFAP-, and iNOS-positive cells were counted for 10 non-overlapping random views (Figure 4). After 7, 14, and 28 d of injection, the number of TH-positive cells decreased, but the number of GFAP- and iNOS-positive cells increased significantly compared with that in the contralateral brain and the saline-treated lateral brain.

Dopamine (DA) is an important central neurotransmitter involved in the regulation of neuropsychiatric activities. The central substantia nigra DA system is the major center of the extrapyramidal system of motor functions. DA dysfunction can lead to serious neurological and psychiatric disorders, thereby causing behavioral changes. Mn-nanoparticles induce apoptosis in dopaminergic neuronal cells *in vitro* [30] and may involve mechanisms associated with neurodegeneration [31]. Other nanomaterials, such as silica, can decrease dopamine concentrations in the striatum and impair dopaminergic neurons [32]. In another study, dopamine-related gene expression is altered in cultured PC12 cells after exposure to Ag and Cu nanoparticles [31]. Our results showed that TH is expressed at a less extent in the nano-MnO<sub>2</sub>-injected side of the midbrain than in the saline-treated contralateral, which is consistent with the *in vitro* tests of Mn-nanoparticles. It is indicated that Mn-nanoparticles induced dopaminergic neuronal impairment *in vivo* and this can explain the changes in the motor behavior of rats, however, when compared with the positive control, 6-OHDA injected rats, the dopaminergic neuron dysfunction is still at early stage, for no head-to tail rotation is observed.

**Figure 1.** TH immunohistochemical staining of rat midbrain. (A) Damaged side of nano-MnO<sub>2</sub> group (40×), Bar = 500 μm; (B) damaged side of nano-MnO<sub>2</sub> group (400×), Bar = 50 μm; (C) uninjured side of nano-MnO<sub>2</sub> group (400×), Bar = 50 μm; (D) damaged side of 6-OHDA group (40×), Bar = 500 μm; (E) damaged side of 6-OHDA group (400×), Bar = 50 μm; (F) uninjured side of 6-OHDA group (400×), Bar = 50 μm; (G) damaged side of saline group (40×), Bar = 500 μm; H: damaged side of saline group (400×), Bar = 50 μm; and I: uninjured side of saline group (400×), Bar = 50 μm.



iNOS expression in the damaged sides is significantly higher than that in the contralaterals. This result may be associated with inflammatory reaction after nano-MnO<sub>2</sub> stimulation. Inflammation is one of the major bioeffects of nanomaterials in organisms [33–35]. The astrocytes derived iNOS can synthesize large amounts of NO and on a slower time scale [36]. NO is secreted as free radicals and is a critical mediator of inflammation in pathological processes [37]. Excessive NO mediates neurological toxicity and cytotoxicity, thereby causing tissue damage; furthermore, excessive NO directly or indirectly induces neuronal impairment [38].

GFAP is the main component of the collagen in an astrocyte body; GFAP is slightly or negatively expressed in a normal brain. Astrocytes are rapidly transformed to an activated state when the brain tissue is damaged; as a result, the number of cells and GFAP expression are significantly increased. Activated astrocytes then function to protect and induce toxicity on neurons; this dual function is called a double-edged effect [39]. GFAP expression in the damaged side of the hippocampus was upregulated significantly compared with that in the contralateral and damaged side of the saline-treated rats. This result indicated that nano-MnO<sub>2</sub> increased astrocyte activity. Changes in the inner environments of the hippocampus may also affect the memory ability of nano-MnO<sub>2</sub>-injected rats.

**Figure 2.** GFAP immunohistochemical staining of the hippocampus of rats (400 $\times$ , Bar = 50  $\mu$ m). (A) Damaged side, nano-MnO<sub>2</sub> group; (B) uninjured side, nano-MnO<sub>2</sub> group; (C) damaged side, 6-OHDA group; (D) uninjured side, 6-OHDA group; (E) damaged side, saline group; and (F) uninjured side, saline group.

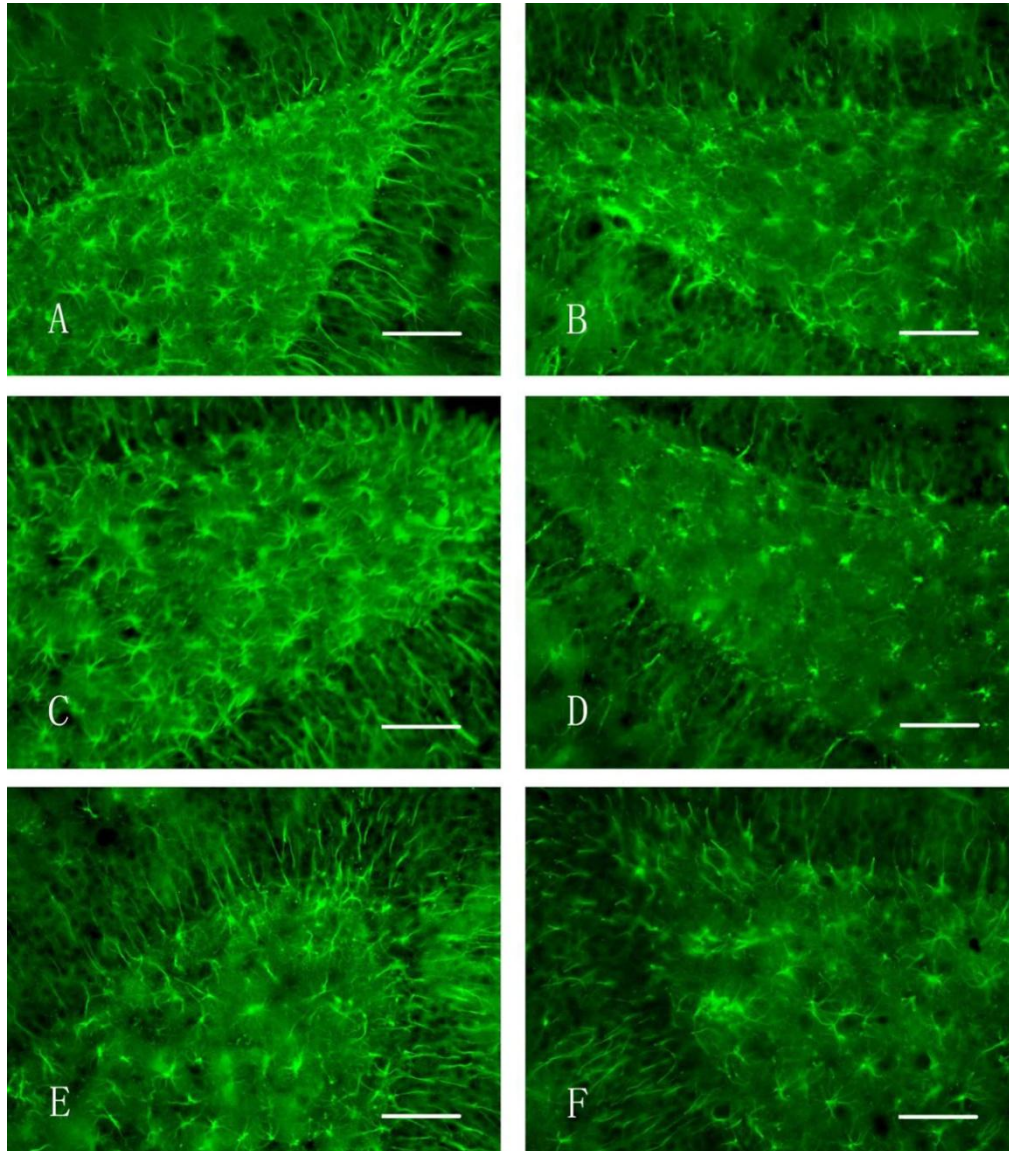


**Figure 3.** iNOS immunohistochemical staining of the midbrain of rats (400×, Bar = 50 μm). (A) Damaged side, nano-MnO<sub>2</sub> group; (B) uninjured side, nano-MnO<sub>2</sub> group; (C) damaged side, 6-OHDA group; (D) uninjured side, 6-OHDA group; (E) damaged side, saline group; and (F) uninjured side, saline group.

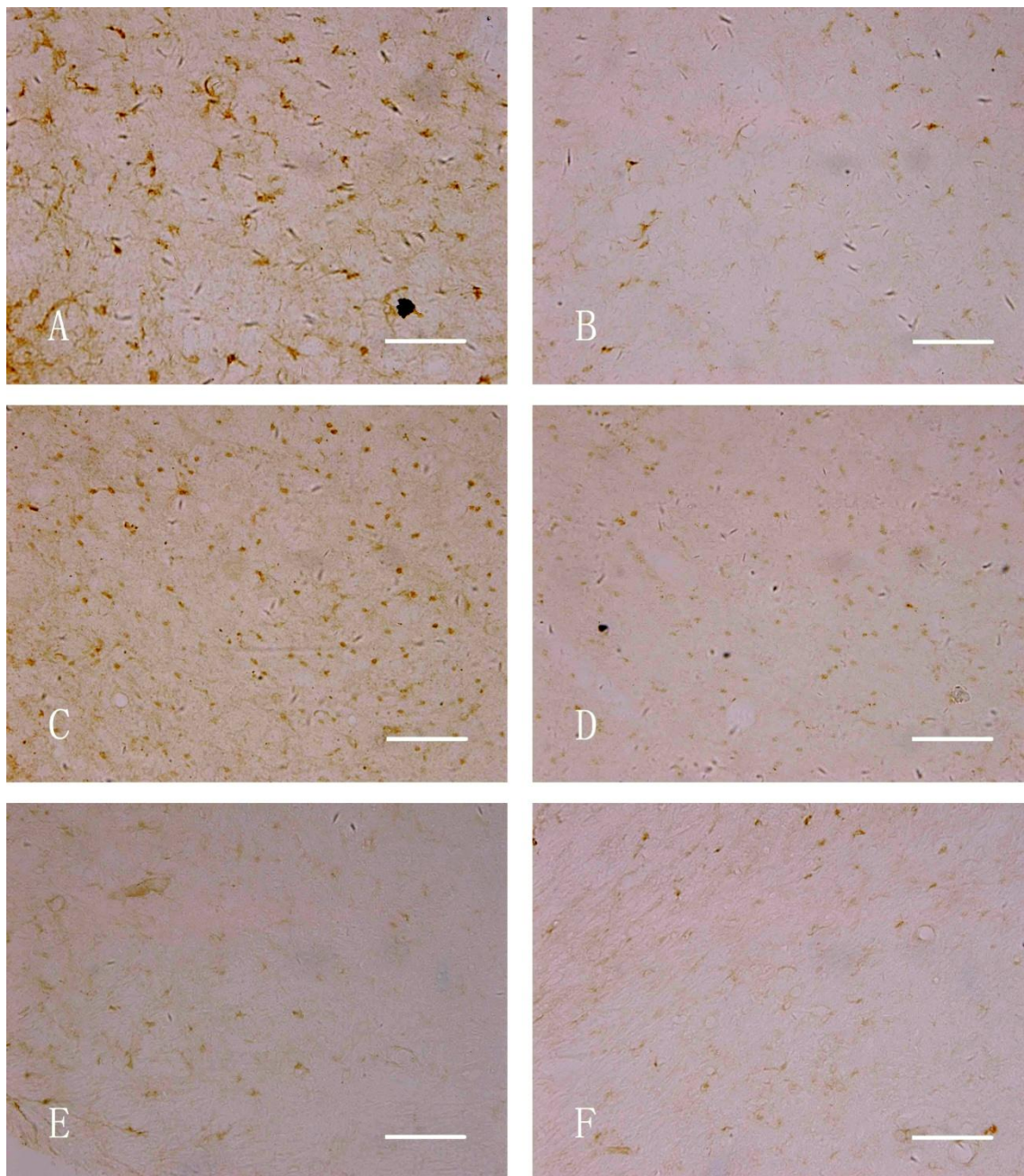
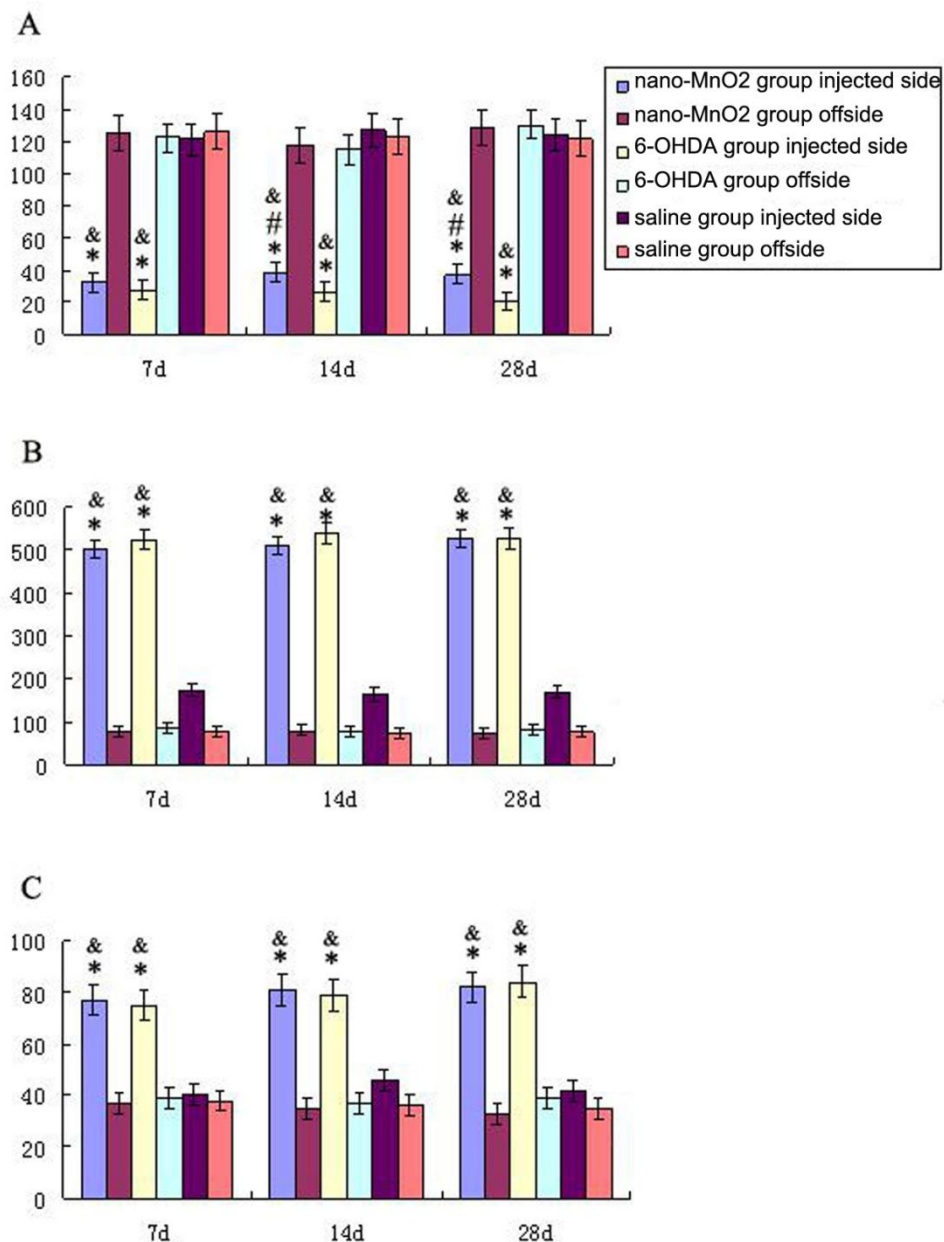


**Figure 4.** Number of immunostained positive cells in both sides of rat brain. (A) TH-positive cells, (B) GFAP-positive cells; and (C) iNOS-positive cells (\*  $p < 0.05$  compared with saline injected side, #  $p < 0.05$  compared with 6-OHDA injected side, &  $p < 0.05$  compared with contralateral).



#### 4. Conclusions

In summary, our results showed that nano-MnO<sub>2</sub> injected intracerebrally in the rat brain induced changes in the locomotor and spatial memory abilities of rats, which is associated with dopaminergic neuronal impairment and MnO<sub>2</sub> nanoparticle-induced inflammation. When compared with the positive control, 6-OHDA, MnO<sub>2</sub> nanoparticles only induced the early stage symptoms of extrapyramidal impairment with a selective loss of dopaminergic neurons, however, considering the potential use of

MnO<sub>2</sub> nanoparticles in diagnosis or treatment procedures, a proper dose should be carefully selected to avoid potential neurotoxic effects.

### Acknowledgments

This study was supported by the National Natural Science Foundation of China (NSFC No. 30901167), the State Key Program for Basic Research of China (Grant No. 2011CB933404), the Opening Foundation of Key Laboratory of Environmental Medicine Engineering of Ministry of Education, China (Grant No. 2010EME008), and the Fundamental Research Funds for the Central Universities.

### Author Contributions

Conception and design: Tao Li, Tingting Shi, Shuilin Zeng; Data collection: Tao Li, Tingting Shi; Writing the article: Xiaobo Li; Statistical analysis: Tao Li, Tingting Shi; Obtained funding: Tao Li, Xiaobo Li, Lihong Yin; Overall responsibility: Pu Yuepu.

### Conflicts of Interest

The authors declare no conflict of interest.

### References

1. Post, J.E. Manganese oxide minerals: Crystal structures and economic and environmental significance. *Proc. Natl. Acad. Sci.* **1999**, *96*, 3447–3454.
2. Address, K.J.; Basilion, J.P. Structure and dynamics of the iron responsive element RNA: Implications for binding of the RNA by iron regulatory binding proteins. *J. Mol. Biol.* **1997**, *274*, 72–83.
3. Aschner, M.; Gannon, M. Manganese uptake and efflux in cultured rat astrocytes. *J. Neurochem.* **1992**, *58*, 730–735.
4. Fitsanakis, V.A.; Aschner, M. The importance of glutamate, glycine, and gamma-aminobutyric acid transport and regulation in manganese, mercury and lead neurotoxicity. *Toxicol. Appl. Pharmacol.* **2005**, *204*, 343–354.
5. Liao, S.L.; Chen, C.J. Manganese stimulates stellation of cultured rat cortical astrocytes. *Neuroreport* **2001**, *12*, 3877–3881.
6. Calne, D.B.; Chu, N.S. Manganism and idiopathic parkinsonism: Similarities and differences. *Neurology* **1994**, *44*, 1583–1586.
7. Cersosimo, M.G.; Koller, W.C. The diagnosis of manganese-induced parkinsonism. *Neurotoxicology* **2006**, *27*, 340–346.
8. Olanow, C.W. Manganese-induced parkinsonism and Parkinson's disease. *Ann. N. Y. Acad. Sci.* **2004**, *1012*, 209–223.
9. Sousa, F.; Mandal, S. Functionalized gold nanoparticles: A detailed *in vivo* multimodal microscopic brain distribution study. *Nanoscale* **2010**, *2*, 2826–2834.

10. Zhang, Q.L.; Li, M.Q. *In vivo* toxicity of nano-alumina on mice neurobehavioral profiles and the potential mechanisms. *Int. J. Immunopathol. Pharmacol.* **2011**, *24*, S23–S29.
11. Ragupathy, P.; Vasan, H.N. Synthesis and characterization of Nano-MnO<sub>2</sub> for electrochemical supercapacitor studies. *J. Electrochem. Soc.* **2008**, *155*, A34–A40.
12. Jothiramalingam, R.; Wang, M.K. Synthesis, characterization and photocatalytic activity of porous manganese oxide doped titania for toluene decomposition. *J. Hazard. Mater.* **2007**, *147*, 562–569.
13. Felton, C.; Karmakar, A. Magnetic nanoparticles as contrast agents in biomedical imaging: Recent advances in iron- and manganese-based magnetic nanoparticles. *Drug Metab. Rev.* **2014**, *46*, 142–154.
14. Kurokawa, A.; Yanoh, T. Preparation and magnetic properties of multiferroic CuMnO<sub>2</sub> nanoparticles. *J. Nanosci. Nanotechnol.* **2014**, *14*, 2553–2556.
15. Antonini, J.M.; Afshari, A.A. Design, construction, and characterization of a novel robotic welding fume generator and inhalation exposure system for laboratory animals. *J. Occup. Environ. Hyg.* **2006**, *3*, 194–203.
16. Long, Z.; Jiang, Y.M. Vulnerability of welders to manganese exposure—A neuroimaging study. *Neurotoxicology* **2014**, *3*, doi: 10.1016/j.neuro.2014.03.007.
17. Hu, Y.L.; Gao, J.Q. Potential neurotoxicity of nanoparticles. *Int. J. Pharm.* **2010**, *394*, 115–121.
18. Lucchini, R.G.; Guazzetti, S. Neurofunctional dopaminergic impairment in elderly after lifetime exposure to manganese. *Neurotoxicology* **2014**, *5*, doi: 10.1016/j.neuro.2014.05.006.
19. Gerber, G.B.; Leonard, A. Carcinogenicity, mutagenicity and teratogenicity of manganese compounds. *Crit. Rev. Oncol. Hematol.* **2002**, *42*, 25–34.
20. Gonzalez-Cuyar, L.F.; Nelson, G. Quantitative neuropathology associated with chronic manganese exposure in South African mine workers. *Neurotoxicology* **2013**, *12*, doi:10.1016/j.neuro.2013.12.008.
21. Benedetto, A.; Au, C. Manganese-induced dopaminergic neurodegeneration: Insights into mechanisms and genetics shared with Parkinson's disease. *Chem. Rev.* **2009**, *109*, 4862–4884.
22. Riquelme, E.; Abarca, J. An NR2B-dependent decrease in the expression of trkB receptors precedes the disappearance of dopaminergic cells in Substantia Nigra in a rat model of Presymptomatic Parkinson's Disease. *Parkinson's Dis.* **2012**, *2012*, doi:10.1155/2012/129605.
23. Albani, S.H.; McHail, D.G. Developmental studies of the hippocampus and hippocampal-dependent behaviors: Insights from interdisciplinary studies and tips for new investigators. *Neurosci. Biobehav. Rev.* **2014**, *43C*, 183–190.
24. Frank, L.M.; Brown, E.N. Hippocampal and cortical place cell plasticity: Implications for episodic memory. *Hippocampus* **2006**, *16*, 775–784.
25. Holahan, M.R.; Routtenberg, A. Lidocaine injections targeting CA3 hippocampus impair long-term spatial memory and prevent learning-induced mossy fiber remodeling. *Hippocampus* **2011**, *21*, 532–540.
26. Blecharz-Klin, K.; Piechal, A. Effect of intranasal manganese administration on neurotransmission and spatial learning in rats. *Toxicol. Appl. Pharmacol.* **2012**, *265*, 1–9.
27. Fitsanakis, V.A.; Thompson, K.N. A chronic iron-deficient/high-manganese diet in rodents results in increased brain oxidative stress and behavioral deficits in the morris water maze. *Neurotox. Res.* **2009**, *15*, 167–178.

28. Xie, Y.; Wang, Y. Effects of nanoparticle zinc oxide on spatial cognition and synaptic plasticity in mice with depressive-like behaviors. *J. Biomed. Sci.* **2012**, *19*, doi:10.1186/1423-0127-19-14.
29. Mohammadipour, A.; Hosseini, M. The effects of exposure to titanium dioxide nanoparticles during lactation period on learning and memory of rat offspring. *Toxicol. Ind. Health* **2013**, *9*, doi:10.1177/0748233713498440.
30. Afeseh Ngwa, H.; Kanthasamy, A. Manganese nanoparticle activates mitochondrial dependent apoptotic signaling and autophagy in dopaminergic neuronal cells. *Toxicol. Appl. Pharmacol.* **2011**, *256*, 227–240.
31. Wang, J.; Rahman, M.F. Expression changes of dopaminergic system-related genes in PC12 cells induced by manganese, silver, or copper nanoparticles. *Neurotoxicology* **2009**, *30*, 926–933.
32. Wu, J.; Wang, C. Neurotoxicity of silica nanoparticles: Brain localization and dopaminergic neurons damage pathways. *ACS Nano* **2011**, *5*, 4476–4489.
33. Lee, J.K.; Sayers, B.C. Multi-walled carbon nanotubes induce COX-2 and iNOS expression via MAP kinase-dependent and -independent mechanisms in mouse RAW264.7 macrophages. *Part. Fibre Toxicol.* **2012**, *9*, doi:10.1186/1743-8977-9-14.
34. Gojova, A.; Guo, B. Induction of inflammation in vascular endothelial cells by metal oxide nanoparticles: Effect of particle composition. *Environ. Health Perspect.* **2007**, *115*, 403–409.
35. Muller, L.; Riediker, M. Oxidative stress and inflammation response after nanoparticle exposure: Differences between human lung cell monocultures and an advanced three-dimensional model of the human epithelial airways. *J. R. Soc. Interface* **2009**, *7*, S27–S40.
36. Buskila, Y.; Abu-Ghanem, Y. Enhanced astrocytic nitric oxide production and neuronal modifications in the neocortex of a NOS<sub>2</sub> mutant mouse. *PLoS One* **2007**, *2*, doi:10.1371/journal.pone.0000843.
37. Tieu, K.; Ischiropoulos, H. Nitric oxide and reactive oxygen species in Parkinson's disease. *IUBMB Life* **2003**, *55*, 329–335.
38. Stevenson, L.; Matesanz, N. Reduced nitro-oxidative stress and neural cell death suggests a protective role for microglial cells in TNFalpha<sup>-/-</sup> mice in ischemic retinopathy. *Investig. Ophthalmol. Vis. Sci.* **2010**, *51*, 3291–3299.
39. Shiratsuch, H.; Basson, M.D. Differential regulation of monocyte/macrophage cytokine production by pressure. *Am. J. Surg.* **2005**, *190*, 757–762.